

Supplementary Material for

Evaluation of aerosol- and gas-phase tracers for identification of transported biomass burning emissions in an industrially influenced location in Texas, USA

5 Sujan Shrestha¹, Shan Zhou^{2,3}, Manisha Mehra¹, Meghan C. Guagenti¹, Subin Yoon², Sergio L. Alvarez², Fangzhou Guo^{2,3}, Chun-Ying Chao³, James H. Flynn III², Yuxuan Wang², Robert J. Griffin^{3,4}, Sascha Usenko¹, Rebecca J. Sheesley¹

¹Department of Environmental Science, Baylor University, Waco, TX, USA

²Department of Earth and Atmospheric Sciences, University of Houston, Houston, TX, USA

³Department of Civil and Environmental Engineering, Rice University, TX, USA

10 ⁴School of Engineering, Computing, and Construction Management, Roger Williams University, Bristol, RI, USA
Correspondence to: Rebecca J. Sheesley (Rebecca_Sheesley@baylor.edu)

1. Equivalent BC (eBC) calculation

Filter-based optical techniques of black carbon (BC) measurement do not measure the mass concentration directly but uses Mie theory to measure the light absorption coefficient of particles. The absorption coefficients (σ_{abs}) are converted into an equivalent mass concentration (eBC) using mass absorption cross section (MAC) (equation (1) below). Field based studies have shown a large variability in MAC values ranging from $1.6 \text{ m}^2\text{g}^{-1}$ to $28.3 \text{ m}^2\text{g}^{-1}$ at 550 nm (Sharma et al., 2002; Bond and Bergstrom, 2006). Large temporal and spatial variability in MAC value reported in previous studies is due to different mixing states of BC. Once emitted into the atmosphere these particles are subject to several coating processes with layers of other organic and inorganic materials (Zhao et al., 2021; Bond and Bergstrom, 2006). The coating over a core BC enhances the aerosol absorption by acting as a lens that helps in focusing more incident light on the enclosed BC core (a phenomena known as “lensing effect”) (Fuller et al., 1999). This results into higher MAC value of the coated BC. Bond and Bergstrom (2006) reported MAC value of $7.5 \pm 1.2 \text{ m}^2\text{g}^{-1}$ at 550 nm for a fresh uncoated particle. But due to coating over fresh BC during local and long-range transport, the absorption can be enhanced by up to 100% (Schwarz et al., 2008; Bond and Bergstrom, 2006). Some of the commercially available instruments, however, use a fixed MAC values to obtain BC concentration, e.g., an aethalometer uses $7.77 \text{ m}^2\text{g}^{-1}$ at 880 nm or $13.14 \text{ m}^2\text{g}^{-1}$ at 520 nm (Drinovec et al., 2015). Use of fixed MAC values is convenient when additional collocated measurements required for MAC calculation are not available but this approach remains debatable (Zhao et al., 2021)

$$\text{eBC } (\mu\text{g m}^{-3}) = \frac{\sigma_{\text{abs}} (\text{Mm}^{-1})}{\text{MAC } (\text{m}^2\text{g}^{-1})} \quad [1]$$

During the field measurement in Port Aransas, σ_{abs} was measured using Tri-color Absorption Photometer (TAP) through a $\text{PM}_{2.5}$ cyclone at three wavelengths: 365 nm, 520 nm and 640nm. Operational detail about TAP are presented elsewhere (Bernardoni et al., 2021; Ogren et al., 2017). In addition to aerosol optical measurement, a $\text{PM}_{2.5}$ bulk filter sampler was operated at Texas A&M Corpus Christi campus which is ~16 miles areal distance apart from the Port Aransas site. During the campaign, a total of six $\text{PM}_{2.5}$ bulk samples were collected. Details about the filter sample are presented in Table S1. The organic and elemental carbon (OC and EC) in the filter samples were measured using Sunset OC EC analyzer using NIOSH protocol (Schauer, 2003). Both Port Aransas and Texas A&M Corpus Christi sites have close proximity to the Gulf of Mexico and received airmasses predominantly from the East and Southeast direction during the campaign. Therefore, it is realistically more appropriate to use the MAC derived as a slope of the linear regression between σ_{abs} from TAP and EC concentration from the $\text{PM}_{2.5}$ filter samples collected during the campaign compared to using literature values. Using this method, the derived MAC at 520 nm was $11.45 \pm 5.32 \text{ m}^2\text{g}^{-1}$ which is slightly lower than that used by aethalometer ($13.14 \text{ m}^2\text{g}^{-1}$). Mathematically, the MAC is given by the following equation:

$$\text{MAC} = \frac{\sigma_{\text{abs}} (\text{Mm}^{-1})}{\text{EC } (\mu\text{gm}^{-3})} \quad [2]$$

where σ_{abs} is the average absorption coefficient measured by TAP at 520 nm during the $\text{PM}_{2.5}$ filter sampling period.

Table S1. Details about PM_{2.5} filter samples collected at Texas A&M Corpus Christi

Sample ID	Start Date	Start Time	End Date	End Time
210403_MV2.5_COR	4/3/21	10:06	4/6/21	17:02
210406_MV2.5_COR	4/6/21	19:19	4/9/21	18:43
210409_MV2.5_COR	4/9/21	18:59	4/13/21	11:41
210413_MV2.5_COR	4/13/21	11:48	4/16/21	18:21
210416_MV2.5_COR	4/16/21	18:38	4/20/21	17:01
210420_MV2.5_COR	4/20/21	17:07	4/22/21	11:34

50

Table S2. The 1-min and 2.5-min minimum detection limits (MDL) of the measured nonrefractory submicron aerosol species during the sampling campaign, which were determined as three times the standard deviation (3σ) of the corresponding signals in particle-free ambient air.

Species	MDL- 2.5 min ($\mu\text{g m}^{-3}$)
Organics	0.37
Sulfate	0.072
Nitrate	0.02
Ammonium	0.063
Chloride	0.024

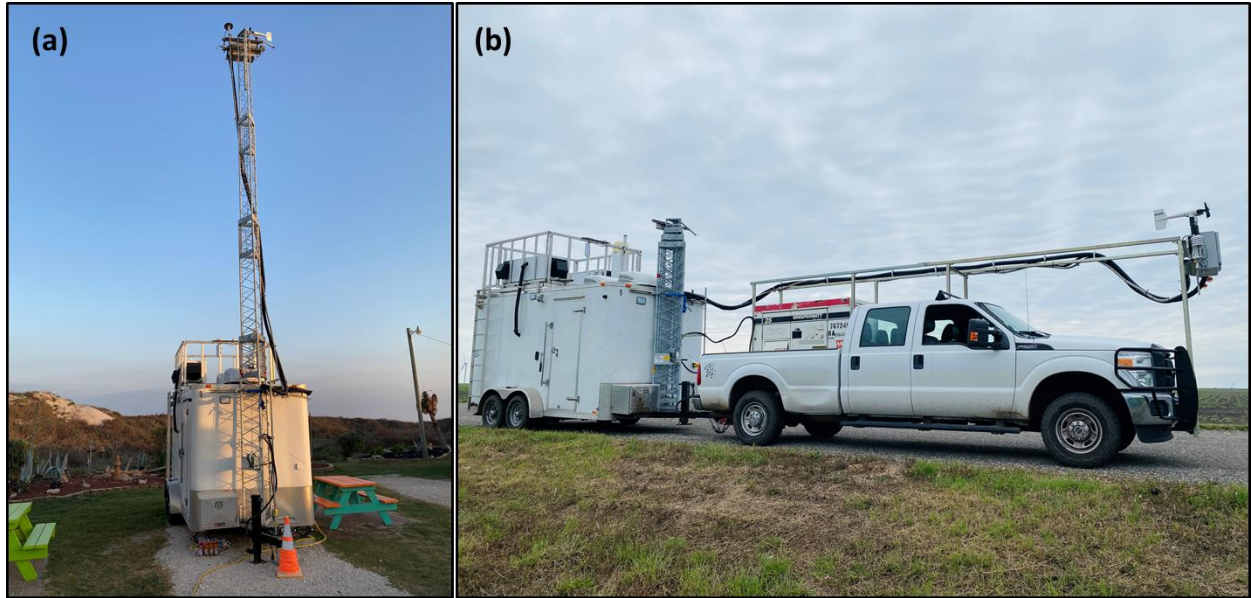
Table S3. Minimum detection limit (MDL) for 30-s averaged data and associated uncertainty for trace gas measurements.

Species	Uncertainty (%)	MDL (ppbv)
CO	1.4	0.13
CO ₂	1	0.33
NO	4.7	0.07
NO	4.5	0.35
NO ₂	5.4	0.13
NO ₂	9.3	0.49
NO _y	5.6	0.48
O ₃	1.9	0.23
SO ₂	9.1	0.92

55 **Table S4.** Minimum detection limit (MDL) in ppbv and uncertainty associated with the measured VOCs during the sampling campaign.

Species	m/z	Uncertainty (%)	MDL (ppbv)
Formaldehyde	31	10.8	0.66
Acetonitrile	42	10.7	0.09
Acetaldehyde	45	9.6	0.26
Acetone	59	20.9	0.42
DMS	63	9.6	0.15
Isoprene	69	10.1	0.15
MVK+MACR	71	9.5	0.16
MEK	73	9.6	0.12
Benzene	79	9.9	0.13
Toluene	93	9.9	0.16
Monoterpene	137	11.2	0.52
Hydroxyacetone	75	16.7	0.44
Styrene	105	11.4	0.1
Xylene	107	11.1	0.18

Figures



60

Fig. S1. Mobile air quality laboratory (MAQL2) during (a) stationary phase and (b) mobile phase.

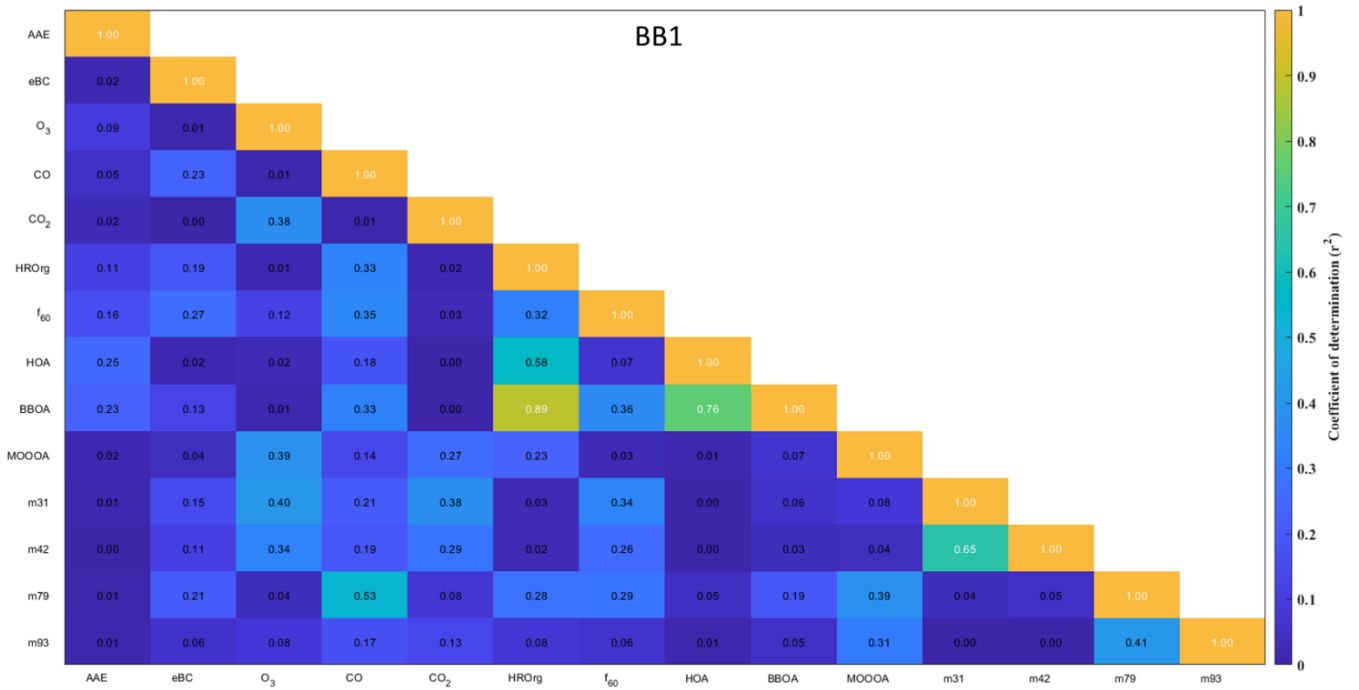
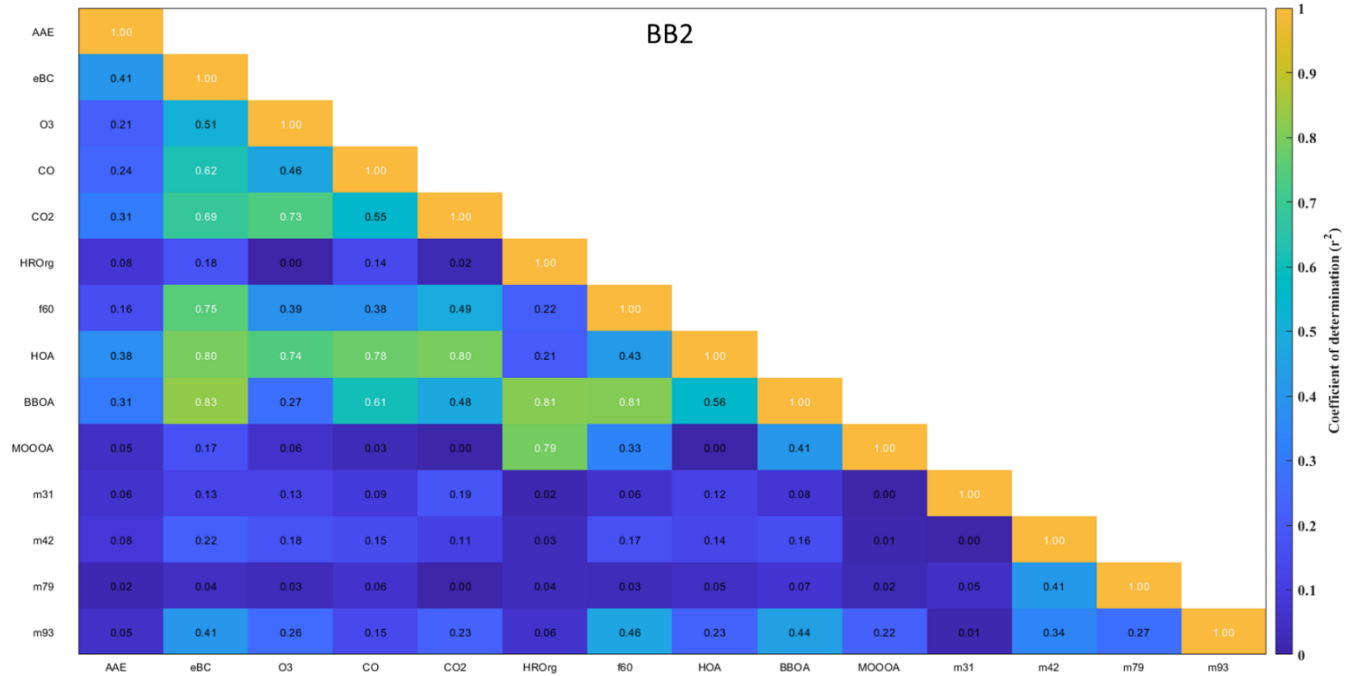
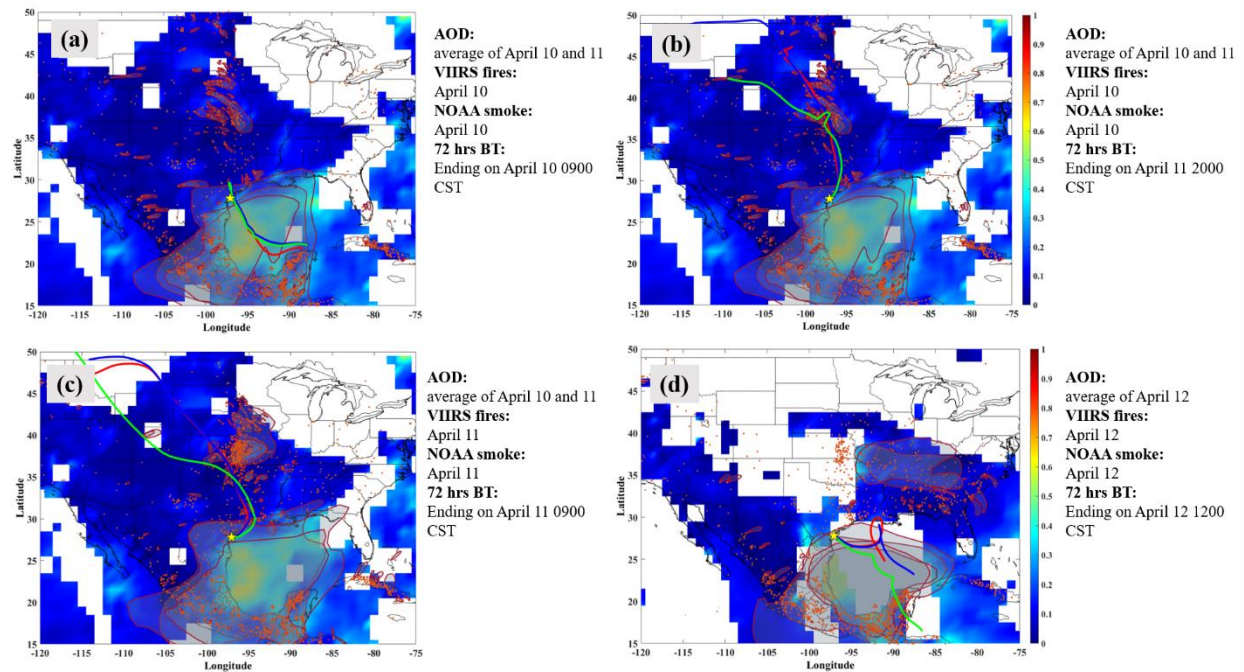


Fig. S2. Correlation plot of select-aerosol optical properties, trace gases, aerosol composition and VOCs during BB1.



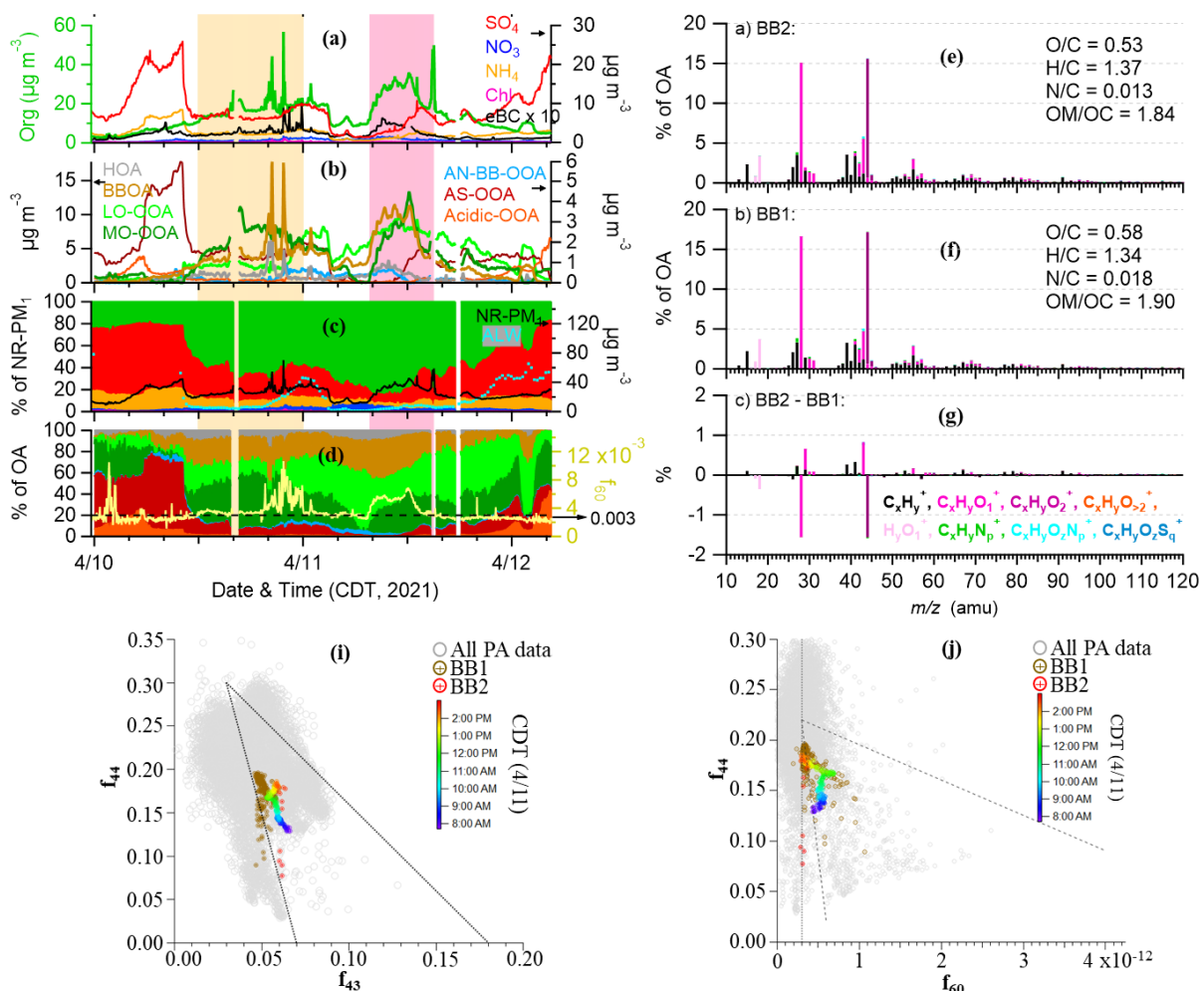
65

Fig. S3. Correlation plot of select-aerosol optical properties, trace gases, aerosol composition and VOCs during BB2.



70

Fig. S4. Spatial distribution of average Aerosol Optical Depth (AOD) from Aqua and Terra satellites (April 10 – 12, 2021). Visible Infrared Imaging Radiometer Suite (VIIRS) active fire, NOAA Hazard Mapping System (HMS) smoke and HYSPLIT Backward trajectories (BTs) at different starting heights: 50 m (red), 100 m (blue) and 500 m (green) are included in the map. The ending times of the BTs are chosen to show the gradual change in the path of BTs from the Central Mexico to the Northern US during the period of interest in this study. The study site Port Aransas is denoted by a yellow star symbol.

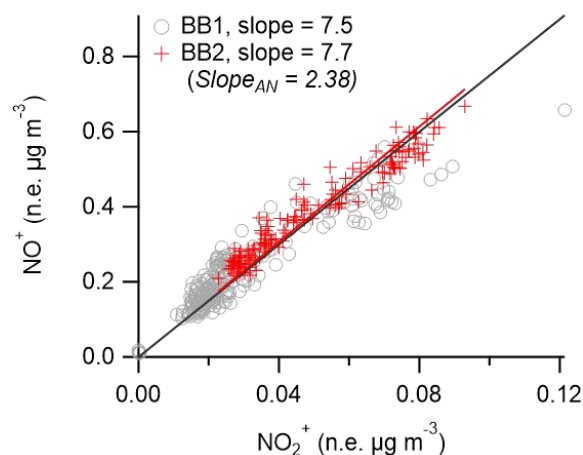


75

80

85

Fig. S5. Time series of (a) mass concentrations of NR-PM₁ species, (b) mass concentrations of OA factors determined from PMF analysis, (c) NR-PM₁ composition, (d) OA composition and f_{60} (i.e., $C_2H_4O_2^+ / OA$) is the yellow lines, and; (e-g) high resolution mass spectra (HRMS) of OA during two BB periods and the difference HRMS colored by eight ion families at $m/z < 120$. The seven PMF factors in panel (b) include: i) hydrocarbon-like organic aerosol (HOA), ii) BB OA (BBOA), iii) less-oxidized oxygenated OA (LO-OOA), iv) more-oxidized OOA (MO-OOA), v) less oxidized OOA associated with ammonium nitrate and biomass burning (AN-BB-OOA), vi) highly oxidized OOA associated with ammonium sulfate (AS-OOA), and vii) highly oxidized OOA associated with acidic sulfate (acidic-OOA). The dashed black line in panel (d) indicates $f_{60} = 0.3\%$. The elemental ratios of OA determined by the Aiken-Ambient method (Aiken et al., 2008) are shown in the legends of panels (e-f). Scatterplot of f_{44} vs. f_{60} (i) and f_{44} vs. f_{60} (j). BB2 data are colored as a function of time of the day. The grey markers correspond to the measured OA during this study. The triangular boundaries set by solid lines (in panel i) and dashed lines (in panel j) represent the ranges observed in ambient OOA field data from literature (Cubison et al., 2011; Ng et al., 2010).



90

Fig. S6. Scatter plot between NO^+ and NO_2^+ measured by the HR-ToF-AMS during BB1 and BB2. Data fitting was performed using orthogonal distance regression.

References

- 95 Aiken, A. C., DeCarlo, P. F., Kroll, J. H., Worsnop, D. R., Huffman, J. A., Docherty, K. S., Ulbrich, I. M., Mohr, C., Kimmel, J. R., Sueper, D., Sun, Y., Zhang, Q., Trimborn, A., Northway, M., Ziemann, P. J., Canagaratna, M. R., Onasch, T. B., Alfarra, M. R., Prevot, A. S. H., Dommen, J., Duplissy, J., Metzger, A., Baltensperger, U., and Jimenez, J. L.: O/C and OM/OC Ratios of Primary, Secondary, and Ambient Organic Aerosols with High-Resolution Time-of-Flight Aerosol Mass Spectrometry, *Environ. Sci. Technol.*, 42, 4478–4485, <https://doi.org/10.1021/es703009q>, 2008.
- 100 Bernardoni, V., Ferrero, L., Bolzacchini, E., Forello, A. C., Gregorič, A., Massabò, D., Močnik, G., Prati, P., Rigler, M., Santagostini, L., Soldan, F., Valentini, S., Valli, G., and Vecchi, R.: Determination of Aethalometer multiple-scattering enhancement parameters and impact on source apportionment during the winter 2017/18 EMEP/ACTRIS/COLOSSAL campaign in Milan, *Atmos. Meas. Tech.*, 14, 2919–2940, <https://doi.org/10.5194/amt-14-2919-2021>, 2021.
- 105 Bond, T. C. and Bergstrom, R. W.: Light absorption by carbonaceous particles: An investigative review, *Aerosol Sci. Technol.*, 40, 27–67, <https://doi.org/10.1080/02786820500421521>, 2006.
- 110 Cubison, M. J., Ortega, A. M., Hayes, P. L., Farmer, D. K., Day, D., Lechner, M. J., Brune, W. H., Apel, E., Diskin, G. S., Fisher, J. A., Fuelberg, H. E., Hecobian, A., Knapp, D. J., Mikoviny, T., Riemer, D., Sachse, G. W., Sessions, W., Weber, R. J., Weinheimer, A. J., Wisthaler, A., and Jimenez, J. L.: Effects of aging on organic aerosol from open biomass burning smoke in aircraft and laboratory studies, *Atmos. Chem. Phys.*, 11, 12049–12064, <https://doi.org/10.5194/acp-11-12049-2011>, 2011.
- Drinovec, L., Močnik, G., Zotter, P., Prévôt, A. S. H., Ruckstuhl, C., Coz, E., Rupakheti, M., Sciare, J., Müller, T., Wiedensohler, A., and Hansen, A. D. A.: The “dual-spot” Aethalometer: An improved measurement of aerosol black carbon with real-time loading compensation, 1965–1979 pp., <https://doi.org/10.5194/amt-8-1965-2015>, 2015.
- 115 Fuller, K. A., Malm, W. C., and Kreidenweis, S. M.: Effects of mixing on extinction by carbonaceous particles, *J. Geophys. Res. Atmos.*, 104, 15941–15954, <https://doi.org/10.1029/1998JD100069>, 1999.
- 120 Ng, N. L., Canagaratna, M. R., Zhang, Q., Jimenez, J. L., Tian, J., Ulbrich, I. M., Kroll, J. H., Docherty, K. S., Chhabra, P. S., Bahreini, R., Murphy, S. M., Seinfeld, J. H., Hildebrandt, L., Donahue, N. M., DeCarlo, P. F., Lanz, V. A., Prévôt, A. S. H., Dinar, E., Rudich, Y., and Worsnop, D. R.: Organic aerosol components observed in Northern Hemispheric datasets from Aerosol Mass Spectrometry, *Atmos. Chem. Phys.*, 10, 4625–4641, <https://doi.org/10.5194/acp-10-4625-2010>, 2010.
- Ogren, J. A., Wendell, J., Andrews, E., and Sheridan, P. J.: Continuous light absorption photometer for long-term studies, *Atmos. Meas. Tech.*, 10, 4805–4818, <https://doi.org/10.5194/amt-10-4805-2017>, 2017.

- 125 Schauer, J. J.: Evaluation of elemental carbon as a marker for diesel particulate matter, *J. Expo. Sci. Environ. Epidemiol.*, 13, 443–453, <https://doi.org/10.1038/sj.jea.7500298>, 2003.
- Schwarz, J. P., Spackman, J. R., Fahey, D. W., Gao, R. S., Lohmann, U., Stier, P., Watts, L. A., Thomson, D. S., Lack, D. A., Pfister, L., Mahoney, M. J., Baumgardner, D., Wilson, J. C., and Reeves, J. M.: Coatings and their enhancement of black carbon light absorption in the tropical atmosphere, *J. Geophys. Res.*, 113, D03203, <https://doi.org/10.1029/2007JD009042>, 2008.
- 130 Sharma, S., Brook, J. R., Cachier, H., Chow, J., Gaudenzi, A., and Lu, G.: Light absorption and thermal measurements of black carbon in different regions of Canada, *J. Geophys. Res. Atmos.*, 107, <https://doi.org/10.1029/2002JD002496>, 2002.
- Zhao, W., Tan, W., Zhao, G., Shen, C., Yu, Y., and Zhao, C.: Determination of equivalent black carbon mass concentration from aerosol light absorption using variable mass absorption cross section, *Atmos. Meas. Tech.*, 14, 1319–1331, <https://doi.org/10.5194/amt-14-1319-2021>, 2021.
- 135